Iranian Journal of Materials Forming 12 (2) (2025) 29-41

IJMF

Online ISSN: 2383-0042

Iranian Journal of Materials Forming

Journal Homepage: http://ijmf.shirazu.ac.ir

Research Article

Designing of Conical Energy Absorber with Internal Pressure by Enhanced Vibrating Particle System Algorithm

A. Mohammadi, M. Sheikhi Azqandi* and S. Rahnama

Department of Mechanical Engineering, University of Birjand, Birjand, Iran

ARTICLE INFO

Article history:

Received 24 February 2025
Reviewed 17 March 2025
Revised 8 May 2025
Accepted 19 May 2025

Keywords:

Conical energy absorber
Finite element method
Collapsing behavior
Meta-heuristic optimization method
Vibrating particle system algorithm

Please cite this article as:

Mohammadi, A., Sheikhi Azqandi, M., & Rahnama, S. (2025). Designing of conical energy absorber with internal pressure by enhanced vibrating particle system algorithm. *Iranian Journal of Materials Forming*, *12*(2), 29-41. https://doi.org/10.22099/IJMF.2025.52548.1327

ABSTRACT

Energy absorbers convert kinetic energy into other forms, including the energy required for plastic deformation. They are designed to minimize damage during collisions and enhance passenger safety. Thin-walled structures—commonly used as energy absorbers—are manufactured in various shapes, such as cylindrical, square, and conical. In this study, three geometrical parameters including the diameter, thickness, and conical apex angle, along with the internal pressure of the absorber prior to deformation, were considered as design variables. The objective was to maximize total energy absorption, which includes both the energy used for plastic deformation and the work done by gas compression inside the absorber. To predict absorber behavior, a full factorial design of experiments (DoE) approach was used. The finite element method was employed to calculate the energy due to plastic deformation and the energy exchange under adiabatic conditions. Additionally, the energy due to gas compression inside the absorber was calculated. Subsequently, the optimal design was identified using the vibrating particle system (VPS) optimization algorithm. The results of the optimal design indicate a 16% increase in energy absorption capability for the conical absorber with internal pressure compared to a similar absorber without internal pressure.

1. Introduction

With the advancement of the transportation systems and the increased likelihood of vehicles colliding with each other or various obstacles, ensuring structural integrity to protect passengers and equipment has become more critical than ever. One solution employed by designers and engineers is the use of energy absorbers, which mitigate a significant portion of the force exerted on a vehicle during an accident. Given the importance of structural weight—particularly in aerospace and air vehicle applications and aerospace structures—minimizing the weight of energy absorbers is a key design consideration. Thin-walled structures are among

* Corresponding author
E-mail address: mojtabasheikhi@birjand.ac.ir (M. Sheikhi Azqandi)
https://doi.org/10.22099/IJMF.2025.52548.1327

the most widely used due to their light weight, low cost, high strength, and excellent energy absorption capabilities, making them valuable tools for engineers designing robust structures [1, 2]. In recent years, a variety of energy absorber designs have been proposed, including column structures [3, 4], sandwich structures [5, 6], plates [7], and honeycomb configurations [8]. These structures undergo deformation under impact loads, dissipating the input energy in the process. Analyzing the collapse behavior of thin-walled structures is essential for accurately assessing their energy absorption capacity and the variation of forces during deformation. Despite significant progress in this area, there remain aspects that require further investigation. This study contributes to that ongoing effort. Azarakhsh et al. [9] investigated the effect of different geometrical parameters on the axial collapse behavior of conical tubes by introducing a flat cap, altering the cross-section, adding vertical and circumferential grooves, as well as internal cavity. They found that conical tubes with caps absorbed more energy than those without; however, their specific energy absorption was lower. Jafarian and Rezvani [10] studied the collapse behavior of multi-part thin-walled cones with and without caps. Their findings suggest that this structure can be effectively employed as a high-performance energy absorber. Suzangarzadeh et al. [11] focused on the optimal design of a multi-section conical aluminum bumper composed of thin-walled segments. In their study, the shock absorber comprised several conical sections with varying thicknesses. Finite element modeling was employed to achieve the optimal design with wall thickness, segment length, and cone apex angles, as design variables. Azarakhsh and Qamarian [12] conducted both experimental and numerical investigations on the energy absorption and deformation of single-walled conical thin-walled tubes subjected to axial and oblique loading. Their study examined the influence of parameters such as apex angle, loading angle, and the inclusion of internal foam on energy absorption performance. Nadaf Eskouei et al. [13] analyzed the collapse of thin-walled conical shells under axial dynamic loading through both experimental testing and numerical simulations. A drop impact device was used for the experiments, while finite element analysis supported the numerical part. All tested samples exhibited a diamond-mode collapse with a quadrangular folding pattern. The results indicated that wall thickness has the most significant influence on the shock absorber's collapse behavior.

In another study, Nadaf Eskouei et al. [14] numerically and experimentally investigated the collapse behavior of thin-walled tubular energy absorbers with a diamond-shaped pattern under axial loading. The studies focused on pipes with one cap and two caps. They observed that the presence of caps reinforced the pipe edges, resulting in greater energy absorption with reduced sag. In addition, they found that the most of the applied kinetic energy was extended the collapse length of the tube. Shariati et al. [15] have explored the buckling behavior and energy absorption capacity of various shell structures, including conical shells, under axial loading through experimental and numerical methods. Their study examined the effects of shock absorber geometry, thickness, height, and the presence and spacing of grooves on buckling load and energy absorption.

Singace and Sobky [16] introduced small wrinkles on the surface of the cylindrical tubes, producing symmetrical collapse in thicker-walled specimens. The effectiveness of this method in enhancing energy absorption was confirmed through experimental results. Song et al. [17] investigated square cross-section absorbers aimed at weight reduction and proposed a design to improve energy absorption while minimizing the initial peak force. Alghamdi [18] classified and analyzed the deformation behavior of thin-walled incomplete conical structures with flat, folded and inward-curved external surfaces using Abaqus software. Tarigopula [19] conducted experimental tests under both static and dynamic loading conditions on thin-walled cylindrical tubes and concluded that stabilizing the upper and lower edges improves energy absorption.

Graciano et al. [20] employed quasi-static testing to assess energy absorbers, determining that both the number and shape of holes in the tube walls significantly

influence the collapse behavior and energy absorption capacity. Alavinia and Liaghat [21] examined thin-walled absorbers with square, circular, rectangular, and hexagonal cross-sections through both experimental and numerical analyses. Their results indicated that circular cross-sections exhibit the highest energy absorption performance. Yob et al. [22] studied thin-walled aluminum tubes with circular and square cross-sections under quasi-static loading, comparing their findings with existing literature. They concluded that circular cross-sections perform approximately 57% better than square ones and can absorb almost twice as much energy.

Sheriff et al. [23] optimized thin-walled conical shells to achieve optimal energy absorption. Geometric parameters such as base diameter, height, and apex angle were considered as design variables. Numerical analysis and experimental impact tests were designed using (DOE). Finally, the effect of different design parameters on energy absorption was analyzed and discussed. Finally, it was found that the thickness and apex angle have the greatest effect on the energy absorption rate. Pirmohammad and Esmaeili [24] analyzed multi-parts geometries and employed neural networks and genetic algorithms to determine the maximum size. Their findings show that a conical structure with a circular cross-section offers superior performance. Abramowicz and Jones [25] examined new failure theories in cylindrical polygonal thin-walled energy absorbers to estimate the average impact force in square sections subjected to vertical force. Alexander et al. [26] studied the collapse behavior of thin-walled cylindrical tubes for the structural design of nuclear fuel tanks. Chirwa [27] conducted both experimental and theoretical investigations into the collapse of aluminum alloy 6063 thin-walled tubes with varying wall thicknesses. Yamazaki and Han [28] simulated the collapse of energy absorbers in symmetric, asymmetric, and Eulerian modes using the finite element method. Their simulations showed strong agreement with experimental results. They then applied the response surface method (RSM) to determine optimal pipe for achieving symmetric collapse. Rahi [29] examined energy absorption and the collapse behavior in circular-square double-walled tubes under axial loading through both numerical and experimental methods. The study also explored the effect of various parameters such as a multi-cell reinforcement and flat caps on energy absorption performance. Elmarakbi et al. [30] investigated the collapse behavior of s-shaped aluminum and steel with different cross-sections. Their results indicated that hexagonal and octagonal geometries exhibited the best energy absorption characteristics. Mokhtarnezhad et al. [31] studied the effect of groove depth and length in grooved pipes. Their simulation revealed that groove length is a critical parameter for achieving controlled collapse in energy absorber design. Wang et al. [32] proposed an innovative design approach that combines the targeted force-displacement (TFD) method with the tailor rolled blank (TRB) process to optimize thin-walled energy-absorbing structures. This methodology, which utilizes topometry optimization, shows great promise for aerospace and automotive applications requiring enhanced energy absorption.

Azarakhsh et al. [33] examined the quasi-static free inversion characteristics of a thin-walled conical tube absorber. This absorber consists of a multi-part conical structure with a spherical end cap, featuring adjustable lengths and diameters designed to optimize energy absorption.

Based on the review of previous studies, the behavior of conical thin-walled energy absorbers under internal pressure has not been thoroughly investigated. Introducing internal pressure has the potential not only to reduce the initial shock upon impact but also to enhance the average force during plastic deformation and, ultimately the overall energy absorption capacity of the absorber. The present study aims to determine the optimal geometric characteristics and initial internal pressure for a conical absorber capable of maximizing energy absorption. To predict absorbers performance, several designs with varying geometric parameters and internal pressure values were first modeled and analyzed using the finite element method. Subsequently, the design of experiments (DoE) approach was employed. Finally, the optimal configuration was identified using the vibrating particle system (VPS) algorithm.

2. Definition of the Problem

Metals absorb impact energy through plastic deformation. The amount of energy absorbed depends on factors such as folding pattern, the geometric shape of the absorber, the material properties, and other influencing parameters. In this research, the finite element method was employed to analyze the problem. Figs. 1(a) and 1(b) illustrate the basic geometrical characteristics of the conical absorber and the meshing approach, as well as placement of the top and bottom caps, respectively.

The deformation of the end caps is significantly less than that of the side walls. Therefore, in this study, the upper and lower caps of the closed conical absorber are modeled as rigid plates. The absorber wall is constructed from extruded aluminum alloy Al 6063-T6. The true stress–strain relationship for this material in the plastic region is provided in Table 1. It is noteworthy that the ultimate strength of the absorber material is 390 MPa [34].

Table 1. True stress-plastic strain data for the aluminum alloy (Al 6063-T6) used in the absorber sidewall [12]

σ_{True} (MPa)	83.3	90.6	94.0	98.2	102.4	104.1
ε_{PI}	0.000	0.051	0.074	0.103	0.143	0.154

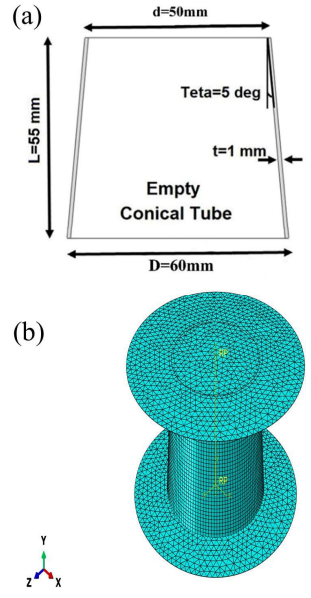

Fig. 1. (a) Geometric characteristics of the conical energy absorber [12], and (b) meshing strategy and placement of the top and bottom caps.

3. Vibrating Particle System Algorithm

Over the past decade, numerous high-performance metaheuristic optimization methods have been developed to address complex engineering problems. These include the Imperialist Competitive Algorithm (ICA) [35], Time Evolutionary Optimization (TEO) [36, 37], and several hybrid metaheuristic techniques such as IDEACO [38], ICACO [39, 40], and GMCBO [41].

Achieving an optimal design for energy absorbers can significantly enhance their energy absorption capacity. To this end, a powerful computational approach is required. In the present study a robust meta-heuristic optimization method inspired by physical principals—known as the vibrating particle system algorithm—was employed. This method was first introduced by Kaveh and Ilchi-Gazan [42]. VPS method is a novel population-based meta-heuristic algorithm modeled on the free vibration of a single-degree-of-freedom system equipped with a viscous damper [43, 44]. In this approach, each solution is treated as a particle striving to reach its equilibrium position. During the optimization process, the algorithm uses physical laws conjunction with stochastic elements to iteratively improve the quality of candidate solutions. The pseudocode of the VPS algorithm is shown in Fig. 2 [44], and a detailed procedural explanation can be found in [45]. To ensure a suitable balance between exploration and exploitation, equilibrium states are derived from both the current population and historically optimal solutions [46]. Three key parameters are defined in the VPS method: HB (Historically Best), representing the best position of the entire population; GB (Good Particle), denoting a good particle; and BP (Bad Particle), indicating a bad particle. For each particle, these parameters are determined as follows: HB is identified as the best candidate up to the current iteration, while GB and BP are randomly chosen from the set of partially optimal and suboptimal solutions, respectively, during each iteration. A parameter P, ranging from 0 to 1, is introduced to control the convergence rate of algorithm [47].

4. Modeling and Problem Analysis

To predict the behavior and energy absorption capacity of the conical absorber under various geometric and mechanical conditions, the design of experiment method was employed. For the effective application of the DoE approach, it is essential to identify the influencing parameters and define the variation range for each design variable. In the case of the conical energy absorber, the most influential factors are the base diameter, wall thickness, and apex angle. The length of the absorber is determined based on installation space constraints and to prevent the occurrence of Euler buckling collapse mode. In this study, the absorber length is fixed at 55 mm for all configurations. Additionally, the introduction of internal pressure within the absorber was investigated as a significant variable. The primary output response is the total energy absorption of the absorber. A fully factorial design method was used for the DoE analysis. Table 2 presents the design variables, the corresponding levels, and the method of variation.

4.1. Finite element analysis

The finite element method (FEM) was used to calculate the energy absorbed through plastic deformation. In this analysis, the upper cap of the absorber is modeled as a rigid, movable, while the other cap is fixed during collapse, constrained with zero degree of freedom. Axial loading is applied centrally to the top cap aligned with the absorber's longitudinal axis. The contact interfaces between the upper and lower surface of the conical absorber and the corresponding caps are defined to prevent any slippage. In practice, the majority of the applied energy is absorbed by the wall, with additional work done by the gas inside the absorber. Therefore, friction effects were not considered in the model, and the applied force remains strictly axial. Due to the use of different materials for the caps and the absorber body, the plastic deformation in the caps is negligible compared to that in the sidewall. For meshing, C3D8R elements were used for the absorbent wall, while R3D3 triangular elements were applied to mesh the rigid cap plates, which are still required to deform for simulation purposes due to their motion. The impact velocity is set at 20 m/s, resulting in a crushing time of 0.005 seconds for a 10 cm deformation of the bumper. To ensure mesh independence and the accuracy of results, a mesh sensitivity analysis was conducted for all sample configurations. Fig. 3 illustrates the percentage variation in absorbed energy between successive mesh refinements for a sample absorber with a base diameter of 100 mm, wall thickness of 2 mm, cone angle of 5°, and internal pressure of 7 bar. In this case, a mesh size of 1 mm yielded an energy deviation of less than 1% compared to the finer 0.5 mm mesh, confirming mesh convergence.

In this study, a large number of conical absorber configurations—each with different values for the design variables—were analyzed to predict absorber behavior during collapse, evaluate the energy absorption capacity, and ultimately identify the optimal design. As a representative case, Fig. 4 shows the deformed shape and the distribution of von Mises equivalent stress at different points of a conical absorber with the specified geometric characteristics.

Fig. 5 presents the force-displacement diagram for a crumple length of 35 mm. In this case, the application of internal pressure results in a reduction of the crushing force at the initial stage of folding.

```
procedure Vibrating Particles System (VPS)
    Initialize algorithm parameters
    Initial positions are created randomly
    The values of objective function are evaluated and HB is stored
    While maximum iterations are not fulfilled
        for each particle
            The GP and BP are chosen
            if P<rand
              w3=0 and w2=1-w1
            end if
            for each component
              New location is obtained
            end for
            Violated components are regenerated by harmony search-based handling
            approach
        end for
        The values of objective function are evaluated and HB is updated
    end while
end procedure
```

Fig. 2. The pseudo of VPS optimization method [44].

Table 2. Design variables and their corresponding levels used for simulating various absorber configurations

Pressure	Apex angle	Thickness	Diameter	Design variables
P (bar)	θ (deg)	t (mm)	D (mm)	
1	3	0.5	60	Levels
5	5	1.0	80	
7	7	1.5	100	
		2.0		

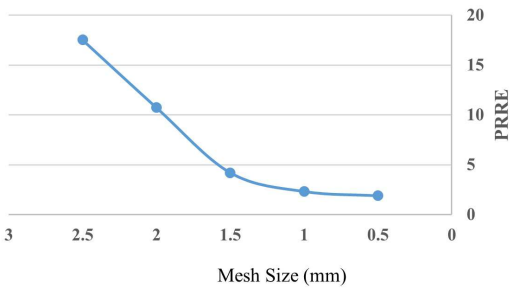

Fig. 3. Percentage of repeated relative error (PRRD) in absorbed energy as a function of mesh size.

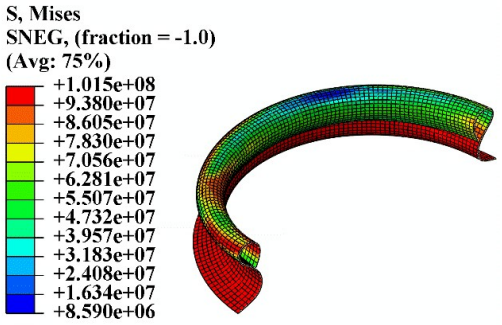

Fig. 4. Deformed shape and distribution of equivalent von Mises stress for a conical absorbent sample with specified geometric parameters.

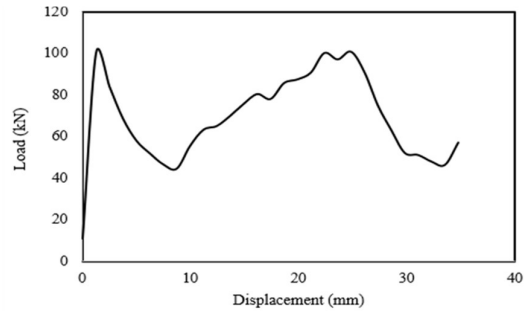

Fig. 5. Force-displacement diagram for a conical absorber with a diameter of 100 mm, wall thickness of 2 mm, cone angle of 5°, and internal pressure of 7 bar.

Fig. 6 illustrates the energy absorbed by the conical absorber over time as a result of the applied force. In this diagram, the horizontal axis represents time, while the vertical axis indicated the amount of energy absorbed. To simplify the problem, it is assumed that the internal pressure remains constant during the deformation of the absorber. Therefore, the energy associated with air compression is calculated separately, as detailed in a subsequent section of this study.

To validate the proposed method, the absorber analyzed in reference [12], with the geometric and mechanical properties specified in Fig. 1 and Table 1, was reevaluated. Fig. 7 presents the force-displacement diagram from both the current research and reference [12]. In this figure, the curves labeled Ref (EX) and Ref (FEM) correspond to the experimental and numerical results reported by Azarakhsh and Qamarian [12], respectively, both of which were obtained under zero internal pressure conditions. The force–displacement curve derived from the present study is shown in black.

Table 3 presents a comparison of the absorbed energy values corresponding to the different methods illustrated in Fig. 7. The percentage of relative error (PRE) in absorbed energy, calculated using Eq. (1), is 1.8 % and 3.6 % for the finite element and experimental methods reported in [12], respectively. These results indicate a high level of agreement and confirm that the simulation approach adopted in the present study

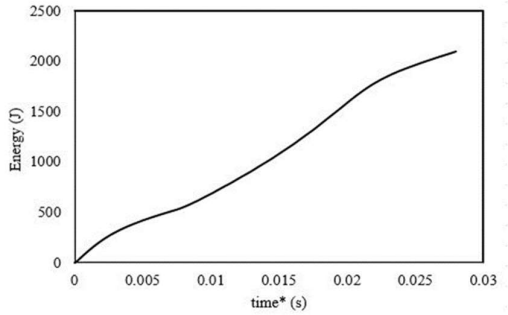

Fig. 6. Energy absorbed by the conical absorber during deformation as a function of time.

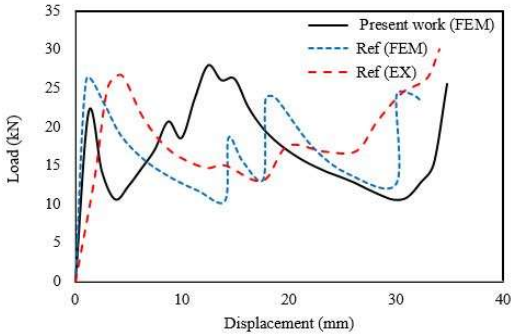

Fig. 7. Comparison of force-displacement curves for the energy absorber between the present study and reference.

Table 3. Percentage of relative error in calculation of absorbed energy

	Present study	FEM [12]	Experimental data [12]
Energy (J)	598	609	620
PRE	-	1.8	3.6

accurately predicts both the collapse behavior and the amount of absorbed energy. To further ensure the reliability of the analysis, an additional simulation was performed for a conical energy absorber with a zero apex angle (i.e., cylindrical absorber) under internal pressure. The results were then compared with those reported in reference [12].

$$PRE = \left(\frac{|E_{pred} - E_E|}{E_E}\right) \times 100 \quad (1)$$

Where E_{pred} and E_E represent the absorbed energy values obtained in the present study and in reference [12], respectively.

In Fig. 8, the deformation of the absorber is compared between the FEM results and the experimental data from reference [12]. The geometric and mechanical specifications are as follows: an aluminum tube (alloy 6063) with an outer diameter of 60 mm, a wall thickness of 1 mm, and a length of 150 mm. The top and bottom cap plates are made of steel. The energy absorption measured experimentally for this adsorber is 333.54 J, while the finite element analysis conducted in this study yielded an absorbed energy of approximately 333.08 J, corresponding to an error of less than 1%.

4.2. Calculation of the energy due to internal air condensation in the absorber

In this study, the energy absorption within the absorber resulting from air compression was calculated using the relations governing an adiabatic process. Eq. (2) computes the work (W) done during the adiabatic process, as the pressure changes from p_1 to p_2 and the volume changes from v_1 to v_2.

Eq. (3) presents the method to calculate the volume of the truncated cone, based on the inner radius r_1, outer radius r_2, and length h. It is assumed that after impact and deformation, the absorber adopts a final shape approximated by a truncated cone with a modified geometric profile. Consequently, the smaller diameter and the length of the absorber are changed. Due to the absorber's airtight closure, the internal pressure varies during deformation. Eq. (4) expresses the relationship between the initial pressure (p_1) and the pressure after deformation (p_2) corresponding to the change in internal volume from v_1 to v_2.

$$W = \left(\frac{1}{1-\gamma}(p_2 v_2 - p_1 v_1)\right) \quad (2)$$

$$v_1 = \frac{1}{3}\pi h(r_1^2 + r_1 r_2 + r_2^2) \quad (3)$$

$$p_2 = p_1\left(\frac{v_1}{v_2}\right)^{\gamma} \quad (4)$$

It is assumed that after deformation, the absorber takes the form of an incomplete cone. Therefore, to calculate the parameter v_2, Eq. (3) is applied again using updated values for r_1 and r_2. As explained in the previous section, the work obtained from Eq. (2) corresponds to the energy required to change the gas volume from v_1 to v_2. Thus, the energy absorbed due to internal air compression within the absorber can be estimated. In this analysis, the interior of the absorber is filled with air. The specific heat ratio γ for air is taken as 1.4, where p_1 represents the initial pressure and v_1 denotes the initial volume of the absorber.

It is further assumed that the folding of the absorber is symmetric during deformation, occurring both inward and outward. In practice, the actual internal volume after deformation is smaller than the estimated volume derived using the truncated cone approximation.

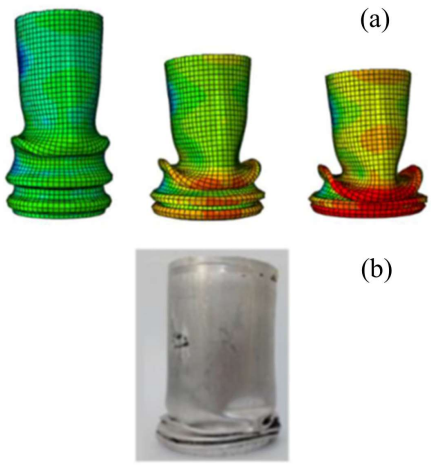

Fig. 8. Comparison of deformation patterns of the conical absorber with a zero-degree apex angle: (a) finite element method, and (b) experimental method.

As a result, the energy calculated based on this simplified model underestimates the true energy absorbed due to air compression. Consequently, the actual work done on the gas and thus the total energy absorption capacity of the desired absorber is greater. This simplification is employed to reduce the complexity associated with accurately calculating the deformed internal volume of the absorber.

5. Results and Discussion

5.1. Effect of design variables on energy absorption

This section evaluates the effect of design parameters on the energy absorption due to plastic deformation (denoted as E_1) and the total absorbed energy considering both plastic deformation and the internal volume change due to pressurization (denoted as $E_1 + E_2$). Fig. 9 shows a Pareto chart showing the relative significance of various design variables on E_1. The most influential parameters on energy absorption from plastic deformation include thickness, diameter, apex angle, and internal air pressure, respectively.

The reciprocal parameter of diameter-thickness also had a significant effect on the amount of energy absorption. The values of the thickness-apex angle, pressure, diameter-apex angle, and apex angle-pressure are omitted due to negligence and an effect of less than 2%.

Based on the Pareto diagram presented in Fig. 10, the effect of different design variables on absorbent energy absorption ($E_1 + E_2$) is respectively in the form of thickness, diameter, internal pressure, the interaction of thickness-diameter, apex angle, and interaction effect the pressure-diameter. The other parameters presented in this figure have no significant effect on the absorption of the total absorbent energy.

It is important to mention that although the application of internal pressure in the absorber in the state (E_1) had the least effect among the main effects on the absorber, due to the amount of energy caused by air compression, internal pressure has a great effect on the absorption of absorbent energy (as can be seen in Fig. 10). Furthermore, the reciprocal double parameter of diameter on pressure is also effective in the amount of energy absorption.

The graphs illustrating the main and interaction effects on E_1 (energy absorption due to plastic deformation) are presented in Figs. 11 and 12, respectively. Similarly, Figs. 13 and 14 depict the main and interaction effects on $E_1 + E_2$ (total energy absorption including plastic deformation and internal volume change). Based on the slope of these graphs, thickness and diameter are identified as the most influential parameters, respectively. A larger diameter results in a greater internal volume, which increases the amount of energy required for air compression during deformation. Consequently, absorbers with larger diameters exhibit higher overall energy absorption.

5.2. Optimal design variables by VPS

The variations range of design variables namely diameter, thickness, apex angle, and internal pressure of the absorber are presented in Table 4. The convergence diagram for the optimal solution obtained through the proposed vibrating particle system optimization algorithm is illustrated in Fig. 15.

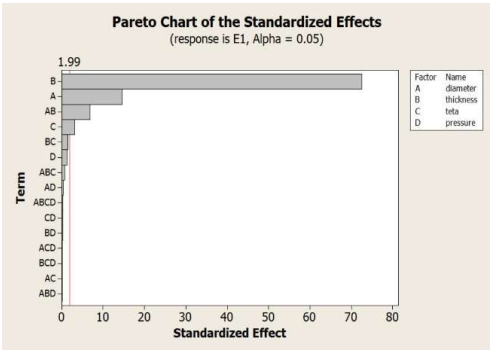

Fig. 9. Pareto diagram of the effects of design variables on energy absorption due to plastic deformation (E_1).

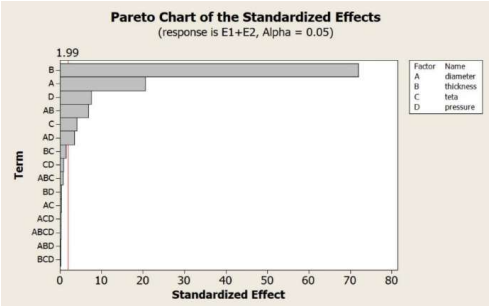

Fig. 10. Pareto diagram of the effects of design variables on total energy absorption, including plastic deformation and internal volume change ($E_1 + E_2$).

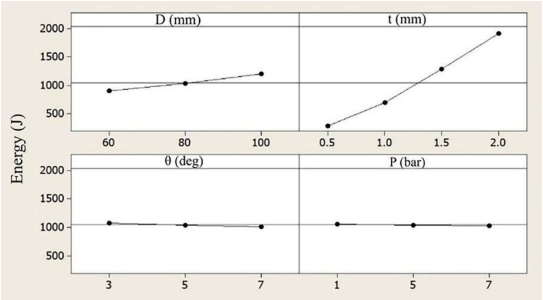

Fig. 11. Main effects of design variables on E_1.

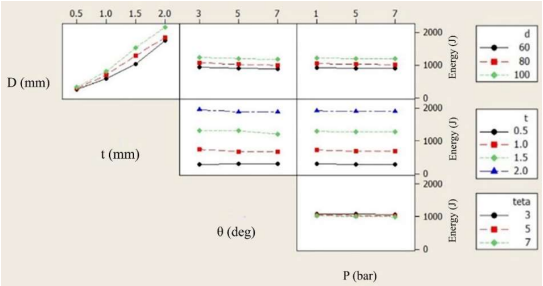

Fig. 12. Interaction effects of design variables on E_1.

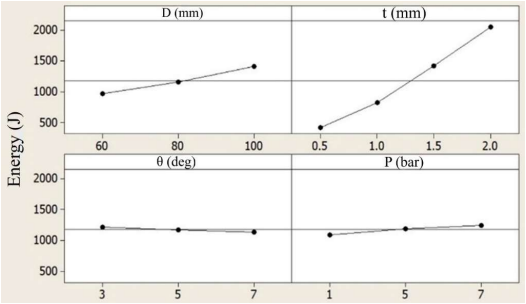

Fig. 13. Main effects of design variables on E_1+E_2.

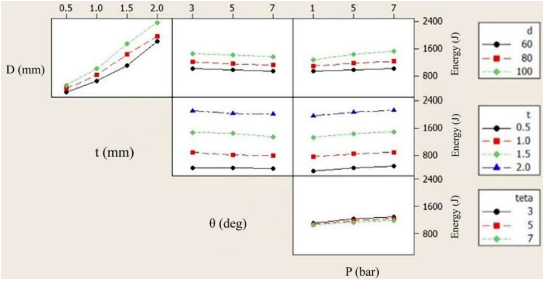

Fig. 14. Interaction effects of design variables on E_1 + E_2.

The VPS method successfully identified the optimal design configuration—outlined in Table 5—within approximately 60 iterations.

Due to the defined limitations in geometrical parameters and internal pressure, the design with a diameter of 100 mm, a thickness of 2 mm, an apex angle of 3 degrees, and an initial pressure of 7 bar was obtained as the optimal configuration.

In Fig. 16, the stress distribution for the optimal design—considering internal pressure and the possibility of condensation are presented and compared with an absorber design without internal pressure and compression effects. Both samples initially had a length of 55 mm and collapsed to 35 mm. The presence of internal pressure altered the collapse mode from an asymmetric (diamond) pattern to a symmetrical state (concertina) pattern, thereby enhancing the energy absorption capacity of the absorber.

In Fig. 17(a) and Fig. 17(b), the energy absorbed over time is shown during the collapse of the adsorber without initial pressure and for the optimized adsorber with initial pressure and air compressibility, respectively. The energy absorbed due to plastic deformation (E_1) in the absorber with internal pressure and compressibility air is 2165 J, whereas for the case without internal pressure and compressibility, it is 2178 J.

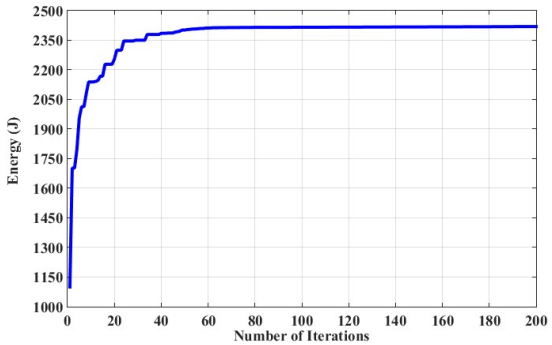

Fig. 15. Convergence curve toward the optimal design using the vibrating particle system (VPS) algorithm.

Table 4. Range limit for diameter, thickness, apex angle, and internal pressure

Design variables	Lower limit	Upper limit
Diameter (mm)	60	100
Thickness (mm)	0.5	2.0
Apex angle (deg)	3.0	7.0
Internal pressure (bar)	1.0	7.0

Table 5. Characteristics of optimum cone absorbent and absorbed energy levels

Diameter (mm)	Thickness (mm)	Apex angle (deg)	Internal pressure (bar)	Absorbed energy (J)
100.00	2.00	3.00	7.00	2415.83

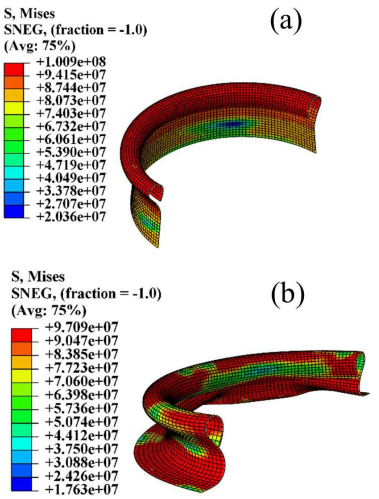

Fig. 16. Effect of air condensation on absorber collapse: (a) without initial pressure and condensation, and (b) with initial pressure and compaction.

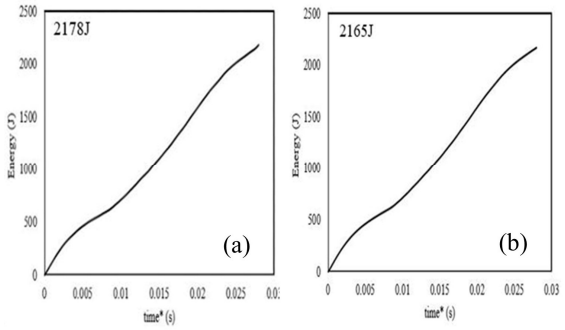

Fig. 17. Energy absorbed: (a) without initial pressure, and (b) with initial pressure.

Although the absorbed with internal pressure shows a slightly lower value of absorbed energy due to plastic deformation, this reduction is because the internal pressure contributes to the deformation process, effectively assisting the collapse and reducing the external force required. The important point is that although the energy absorption capacity is slightly reduced due to normal crushing, the absorber efficiency is higher and it will perform better in complete crumpling. In addition, the energy caused by the change in the volume of the absorber must also be considered.

According to the explanations presented in the previous sections of this research, the volume of the absorbent is equal to the internal volume of the absorber at any moment. The amount of energy required to compress the air during the volume change in collapse (E_2) is 360.9 J. Therefore, the sum of these two energies is the total energy absorbed by the absorber. In this case, the total energy absorbed by the optimized absorber is 2526 J. It should be noted that for an absorber without internal compression and pressure capability, the total energy remains 2178 J. Consequently, the optimized absorber has been able to absorb about 16% more energy than the same model without internal pressure.

Furthermore, an important factor in the design of the absorber is minimizing the initial impact on the occupant. The force-displacement diagram in Fig. 18 shows an initial peak force at the start of impact; however, because the absorber in the current research is compressed in stages, the average force applied increases gradually. As a result, the initial shock is largely mitigated. The graph illustrating the increase in absorbed energy with increasing initial pressure demonstrates how the force required for air compression increases and consequently, the average collapse changes accordingly.

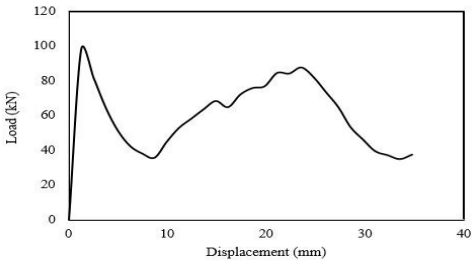

Fig. 18. Force-displacement diagram (showing initial peak).

6. Conclusions

In this research, the optimal design of the geometric characteristics and mechanicals properties of a conical energy absorber was investigated. Based on prior studies on a thin conical wall energy absorber, it is clear that the diameter, wall thickness, and apex angle significantly affect energy absorption. For the first time, this research examined the effect of air pressure inside the shock absorber as an important parameter and confirmed its influence. To predict the absorber's collapse behavior and calculate energy absorption, after validating the method with experimental and numerical results, 108 absorber configurations with different geometric and mechanical conditions were studied using the design of

experiments method. Subsequently, the optimal design was determined using the vibrating particle system optimization method. The optimal design indicates that the innovation presented here not only increases the absorber's efficiency by approximately 16%, but also enhances comfort and safety for mechanical systems occupants. In summary, the key findings are as follows:

- Creating pressure inside the absorber leads to symmetrical or combined collapse modes.
- As internal air pressure increases gradually during collapse, the crushing force also rises progressively, preventing initial shock transmission to occupants.
- By creating air compression inside the absorber during impact, its shock absorption capacity increases.

Conflict of interest

The authors declare no conflict of interest.

Funding

This research has not received any specific funding from any funding organization in the government, commercial, or non-profit sectors.

7. References

[1] Abramowicz, W. (2003). Thin-walled structures as impact energy absorbers. *Thin-Walled Structures, 41*(2), 91-107. https://doi.org/10.1016/S0263-8231(02)00082-4

[2] Ha, N. S., & Lu, G., (2020). Thin-walled corrugated structures: A review of crashworthiness designs and energy absorption characteristics. *Thin-Walled Structures*, *157*, 106995. https://doi.org/10.1016/j.tws.2020.106995

[3] Behrvan, A., SeyyedKashi, H., & Sheikhi Azqandi, M. (2023). Optimal design and manufacturing of a cylindrical damper using time evolutionary optimization method. *Modares Mechanical Engineering*, *23*(1), 45-55. https://doi.org/10.52547/mme.23.1.45

[4] Liu, W., Lin, Z., Wang, N., & Deng, X. (2016). Dynamic performances of thin-walled tubes with star-shaped cross section under axial impact. *Thin-Walled Structures*, *100*, 25–37. https://doi.org/10.1016/j.tws.2015.11.016

[5] Rong, Y., Liu, J., Luo, W., & He, W. (2018). Effects of geometric configurations of corrugated cores on the local impact and planar compression of sandwich panels. *Composites Part B Engineering*, *152*, 324–335. https://doi.org/10.1016/j.compositesb.2018.08.130

[6] Sun, G., Chen, D., Huo, X., Zheng, G., & Li, Q. (2018). Experimental and numerical studies on indentation and perforation characteristics of honeycomb sandwich panels. *Composite Structures, 184*, 110–124. https://doi.org/10.1016/j.compstruct.2017.09.025

[7] Liu, J., Zheng, B., Zhang, K., Yang, B., & Yu, X. (2019). Ballistic performance and energy absorption characteristics of thin nickel-based alloy plates at elevated temperatures. *International Journal of Impact Engineering*, *126*, 160–171. https://doi.org/10.1016/j.ijimpeng.2018.12.012

[8] Yahaya, M. A., Ruan, D., Lu, G., Dargusch, & M. S. (2015). Response of aluminums honeycomb sandwich panels subjected to foam projectile impact–an experimental study. *International Journal of Impact Engineering, 75*, 100–109. https://doi.org/10.1016/j.ijimpeng.2014.07.019

[9] Azarakhsh, S., Qamrian, A., Rizvani, & M. J. (2022). Investigation of different geometric parameters effect on axial crushing of thin-walled conical tubes. *Tabriz Mechanical Engineering, 52*(2), 212-203. https://doi.org/10.22034/jmeut.2022.37017.2596

[10] Jafarian, N., & Rezvani, M. J. (2019). Crushing behavior of multi-component conical tubes as energy absorber: a comparative analysis between end-capped and non-capped conical tubes. *Engineering Structure, 178*, 128–135. https://doi.org/10.1016/j.engstruct.2018.09.092

[11] Souzangarzadeh, H., Rezvani, M. J., & Jahan, A. (2017). Selection of optimum design for conical segmented aluminum tubes as energy absorbers: Application of MULTIMOORA method. *Applied Mathematical Modelling*, *51*, 546-560. https://doi.org/10.1016/j.apm.2017.07.005

[12] Azarakhsh, S., & Ghamarian, A. (2017). Collapse behavior of thin-walled conical tube clamped at both ends subjected to axial and oblique loads. *Thin-Walled Structures*, *112*, 1–11. https://doi.org/10.1016/j.tws.2016.11.020

[13] Nadaf Eskouei, A., Khodarahmi, H., & Sohrabi, M. (2015). Experimental and numerical study of conical thin shells collapse under dynamic axial loadings. *Modares Mechanical Engineering*, *15*(7), 392-402.

[14] Nadaf Eskouei, A., Khodarahmi, H., & Pakian Booshehri, M. (2015). Numerical and experimental study of a diamond collapse of a thin wall tube energy-absorb with caps under dynamic axial loadings. *Modares Mechanical Engineering*, *15*(2), 169-178.

[15] Shariati, M., Davrpaneh, M., Chavshan, H., & Allahbakhsh, H. (2014). Numerical and experimental investigations on buckling and control amount of energy absorption of stainless steel 304L shells with various shapes under axial loading. *Modares Mechanical Engineering*, *14*(3), 60-68.

[16] Singace, A. A., & El-Sobky, H. (1997). Behaviour of axially crushed corrugated tubes. *International Journal of Mechanical Sciences*, *39*(3), 249–268. https://doi.org/10.1016/S0020-7403(96)00022-7

[17] Song, J., Chen, Y., & Lu, G. (2013). Light-weight thin-walled structures with patterned windows under axial crushing. *International Journal of Mechanical Sciences*, *66*, 239–248. https://doi.org/10.1016/j.ijmecsci.2012.11.014

[18] Alghamdi, A. A. A. (2001). Collapsible impact energy absorber: an overview. *Thin-Walled Structures*, *39*(2), 189–213. https://doi.org/10.1016/S0263-8231(00)00048-3

[19] Tarigopula, V., Langseth, M., Hopperstad, O. S., & Clusen, A. H. (2006). Axial crushing of thin-walled high-strength steel sections. *International Journal of Impact Engineering*, *32*(5), 847–882. https://doi.org/10.1016/j.ijimpeng.2005.07.010

[20] Graciano, C., Martínez, G., & Gutiérrez, A. (2012). Failure mechanism of expanded metal tubes under axial crushing. *Thin-Walled Structures*, *51*, 20–24. https://doi.org/10.1016/j.tws.2011.11.001

[21] Alavinia, A., & Liaghat, G. H. (2004). Dynamic crushing of thin-walled columns under impact of projectiles. In *12th Annual International Conference of Mechanical Engineering*, Tarbiat Modarres University, Tehran, Iran.

[22] Yob, M. N., Ismail, K. A., Rojan, M. A., Othman, M. Z., & Ahmad Zaidi, A. M. (2016). Quasi static axial compression of thin-walled aluminum tubes: Analysis of flow stress in the analytical models. *Modern Applied Science*, *10*(1), 34-46. https://doi.org/10.5539/mas.v10n1p34

[23] Mohamed Sheriff, N., Gupta, N. K., Velmurugan, R. & Shanmugapriyan, N. (2008). Optimization of thin conical frusta for impact energy absorption. *Thin-Walled Structures, 46*(6), 653-666. https://doi.org/10.1016/j.tws.2007.12.001

[24] Pirmohammad, S., & Esmaeili Marzdashti, S. (2017). Studying on the collapse behavior of multi-cell conical structures and their optimization using artificial neural network. *Scientific Research Journal of Mechanics of Structures and Fluids, 7*(2), 111-127. https://doi.org/10.22044/jsfm.2017.5577.2363

[25] Abramowicz, W., & Jones, N. (1984). Dynamic axial crushing of square tubes. *International Journal of Impact Engineering, 2*(2), 179–208. https://doi.org/10.1016/0734-743X(84)90005-8

[26] Alexander, J. M. (1960). An approximate analysis of collapse of thin-walled cylindrical shells under axial loading. *Mechanical and Applied Mathematics*, *13*(1), 10-15. https://doi.org/10.1093/qjmam/13.1.10

[27] Chirwa, E. C. (1993). Theoretical analysis of tapered thin-walled metal inverbucktube. *International Journal of Mechanical Sciences*, *35*(3), 325–351. https://doi.org/10.1016/0020-7403(93)90085-9

[28] Yamazaki, K., & Han, J. (2000). Maximization of crushing energy absorption of cylindrical shells. *Advanced Engineering Software*, *31*(6), 425–434. https://doi.org/10.1016/S0965-9978(00)00004-1

[29] Rahi, A. (2018). Controlling energy absorption capacity of combined bitubular tubes under axial loading. *Thin-Walled Structures*, *123*, 222-231. https://doi.org/10.1016/j.tws.2017.11.032

[30] Elmarakbi, A., Long, Y. X., & MacIntyre, J. (2013). Crash analysis and energy absorption characteristics of S-shaped longitudinal members. *Thin-Walled Structures*. *68*, 65–74. https://doi.org/10.1016/j.tws.2013.02.008

[31] Mokhtarnezhad, F., Salehghaffari, S., & Tajdari, M. (2009). Improving the crashworthiness characteristics of cylindrical tubes subjected to axial compression by cutting wide grooves from their outer surface. *International Journal of Crashworthiness*, *14*(6), 601-611. https://doi.org/10.1080/13588260902896466

[32] Wang, Sh., Weigang, A., Lin, T., & Han, X. (2022). Topometry optimization of energy absorbing structure through targeting force-displacement method considering tailor rolled blank process. *International Journal of Aerospace Engineering*, (1), 7776866, https://doi.org/10.1155/2022/7776866

[33] Azarakhsh, S., Rezvani, M. J., Maghsoudpour, A., & Jahan, A. (2024). Inversion performance and multi-objective optimization of multi-component conical energy absorber with a spherical cap. *International Journal of Mechanics and Materials in Design*, *20*, 877–893. https://doi.org/10.1007/s10999-023-09694-1

[34] Ayhan, A. O., Genel, K., & Eksi, S. (2011). Simulation of nonlinear bending behavior and geometric sensitivities for tubular beams with fixed supports. *Thin-Walled Structures*, *51*, 1–9. https://doi.org/10.1016/j.tws.2011.10.016

[35] Sheikhi Azqandi, M., & Ghoddosian, A. (2012). Optimal design of structural support positions using ICA and MFEM. *Modares Mechanical Engineering*, *12*(3), 50-59 (In Persian).

[36] Sheikhi Azqandi, M., Delavar, M, & Arjmand, M. (2016). Time evolutionary optimization: A new meta-heuristic optimization algorithm, In *Proceedings of the 4th International Congress on Civil Engineering, Architecture and Urban Development*, Shahid Beheshti University, Tehran, Iran, (In Persian).

[37] Bijari, Sh., & Sheikhi Azqandi, M. (2022). Optimal design of reinforced concrete one-way ribbed slabs using improved time evolutionary optimization. *International Journal of Optimization in Civil Engineering, 12*(2), 201-214.

[38] Bijari, Sh., & Sheikhi Azqandi, M. (2023). CO_2 emissions optimization of reinforced concrete ribbed slab by hybrid metaheuristic optimization algorithm (IDEACO). *Advances in Computational Design*, *8*(4), 295-307. https://doi.org/10.12989/acd.2023.8.4.295

[39] Safaeifar, H., & Sheikhi Azqandi, M. (2021) Optimal design of the impact damper in free vibrations of SDOF system using ICACO. *International Journal of Optimization in Civil Engineering*, *11*(3), 461-479.

[40] Hassanzadeh, M., & Sheikhi Azqandi, M. (2023). Optimum shape design of axisymmetric extrusion die by using hybrid meta-heuristic optimization (ICACO). *Journal of Solid and Fluid Mechanics, 13*(4), 107-117. https://doi.org/10.22044/jsfm.2023.13213.3749

[41] Sheikhi Azqandi, M. (2021). A novel hybrid genetic modified colliding bodies optimization for designing of composite laminates. *Mechanic Advanced Composite Structures, 8*(1), 203-212. https://doi.org/10.22075/macs.2020.20281.1254

[42] Kaveh, A., & Ilchi Ghazaan, M. (2017). A new meta-heuristic algorithm: vibrating particles system. *Scientia Iranica*, *24*(2), 551-566. https://doi.org/10.24200/sci.2017.2417

[43] Talatahari, S., Jalili, S., & Azizi, M. (2021). Optimum design of steel building structures using migration-based vibrating particles system. *Structures*, *33*, 1394–1413. https://doi.org/10.1016/j.istruc.2021.05.028

[44] Kaveh, A., & Bijari, Sh. (2019). Profile and wave front optimization by metaheuristic algorithms for efficient finite element analysis. *Scientia Iranica*, *26*(4), 2032-2046. https://doi.org/10.24200/sci.2018.20163

[45] Kaveh, A. (2021). *Advances in metaheuristic algorithm for optimal design of structures* (3rd ed.). Springer.

[46] Kaveh, A., & Bijari, Sh. (2018). Simultaneous analysis, design and optimization of trusses via force method structural engineering and mechanics. *Structural Engineering and Mechanics*, *65*(3), 233-241. https://doi.org/10.12989/sem.2018.65.3.233

[47] Kaveh, A., Hoseini Vaez, S. R., & Hosseini, P. (2019). Enhanced vibrating particles system algorithm for damage identification of truss structures. *Scientia Iranica*, *26*(1), 246-256. https://doi.org/10.24200/sci.2017.4265